

Study of the $^{59}\text{Co}(n, \gamma)^{60}\text{Co}$ Reaction and the Level Structure of $^{60}\text{Co}^\dagger$

E. BROOKS SHERA AND D. W. HAFEMEISTER*

Los Alamos Laboratory, University of California, Los Alamos, New Mexico

(Received 6 June 1966)

The level structure of the odd-odd ^{60}Co nucleus has been studied using the thermal-neutron capture reaction $^{59}\text{Co}(n, \gamma)^{60}\text{Co}$. The gamma-ray spectrum from this reaction in the energy intervals 50–1850 keV and 4500–7500 keV has been studied with a Li-drifted Ge spectrometer system. A number of new transitions are reported. The observed levels are compared with those excited by the $^{60}\text{Co}(d, p)$ reaction. Gamma-gamma coincidence measurements using Ge(Li) and NaI detectors have been made, which provide considerable information about the low-energy-level structure. In these measurements a primary high-energy transition, selected by the Ge(Li) detectors, defines a particular low-lying level. The decay of this level, isolated by the coincidence requirement from extraneous background, is observed with a NaI detector. Spins and parities of the excited states below about 1 MeV are deduced from the observed gamma-ray branches. The low-lying excited states are interpreted in terms of the $\pi(f_{7/2})^{-1} \nu(p_{3/2})^{-1}$, $\pi(f_{7/2})^{-1} \nu(f_{5/2})^1$, and $\pi(f_{7/2})^{-1} \nu(p_{1/2})^1$ proton-neutron configurations. The spectra of these configurations, calculated using a zero-range central force for the residual interaction, are compared with the observed levels.

I. INTRODUCTION

THE study of odd-odd nuclei provides information about the residual proton-neutron interaction. In recent years, several studies,^{1–3} both experimental and theoretical, have been made on medium-weight odd-odd nuclei. The present paper reports the results of a study of the $^{59}\text{Co}(n, \gamma)^{60}\text{Co}$ reaction. The odd-odd ^{60}Co nucleus is not populated by beta decay and little has been known concerning its level structure. Previous measurements of the $^{59}\text{Co}(n, \gamma)$ capture gamma-ray spectrum have been reported^{4,5} and the complementary $^{59}\text{Co}(d, p)$ reaction has been studied with a high-resolution spectrograph.⁶ The previous (n, γ) studies have identified a large number of levels, but because of the limited energy resolution available, particularly at low energies, the decay of these levels has been largely unknown. Although the neutron configuration of many of the excited states can be inferred from the value of l_n obtained from the (d, p) angular distribution measurements, no excited-state spin assignments (except for the 58-keV isomer) have been previously proposed.

In the present work, we have studied the neutron-capture gamma-ray spectrum, both at high and low energies, using a Li-drifted Ge detector. In addition, gamma-gamma coincidence measurements have been used to elucidate the low-lying level structure of this nucleus.

II. EXPERIMENTAL PROCEDURE

Spectral Measurements

The gamma-ray spectrum from the $^{59}\text{Co}(n, \gamma)^{60}\text{Co}$ reaction was measured with a Li-drifted Ge spectrometer. This spectrometer, which consists of a Ge(Li) detector placed inside a large NaI annulus (20-cm diam by 30-cm long, with a 6.5-cm-diam bore along its axis), views a target sample placed in the thermal column of the Omega West Reactor. For gamma-ray energies above about 2 MeV, the detection system is operated in the pair mode, which requires that both annihilation quanta be observed in the NaI annulus for an event in the Ge detector to be accepted. This mode effectively suppresses the observation of all but pair-production processes in the Ge detector. For gamma-ray energies less than 2 MeV, the signal from the surrounding NaI annulus is placed in anticoincidence with the Ge detector output to suppress the Compton background.

For the present measurements, a Ge detector with a 3-mm depletion depth was used. This detector, in combination with a field-effect transistor preamplifier, has a resolution (full width at half-maximum) of 2.9 keV at 279 keV and 7.5 keV at 8 MeV. This spectrometer system will be described in greater detail in a future publication.⁷

The target used in these measurements consisted of 200 mg of metallic cobalt. The spectrometer was calibrated using a target consisting of known amounts of Co and melamine. The energies and cross sections of the high-energy transitions in Co were derived from the well-known properties⁸ of the nitrogen lines in melamine. For the energy range below 3 MeV, a series of radioactive sources was employed for energy calibration. The rela-

[†] Work supported by the U. S. Atomic Energy Commission.

* Present address: Carnegie Institute of Technology, Pittsburgh, Pennsylvania.

¹ D. O. Wells, S. L. Blatt, and W. E. Meyerhof, Phys. Rev. **130**, 1961 (1963).

² J. Vervier, Phys. Letters **7**, 200 (1963).

³ Kiyoshi Sasaki, Nucl. Phys. **71**, 95 (1965).

⁴ *Nuclear Data Sheets*, compiled by K. Way *et al.* (Printing and Publishing Office, National Academy of Sciences—National Research Council, Washington 25, D. C., 1963), NRC 20418.

⁵ O. A. Wasson, K. J. Wetzel, and C. K. Bockelman, Phys. Rev. **136**, B1640 (1964).

⁶ H. A. Enge, D. L. Jarrell, and C. C. Angleman, Phys. Rev. **119**, 735 (1960).

⁷ E. T. Journey (to be published).

⁸ H. T. Motz, R. E. Carter, and W. D. Barfield, *Pile Neutron Research in Physics* (International Atomic Energy Agency, Vienna, 1962), p. 234; R. E. Carter and H. T. Motz, Argonne National Laboratory Report ANL-6797, 1963, p. 181 (unpublished).

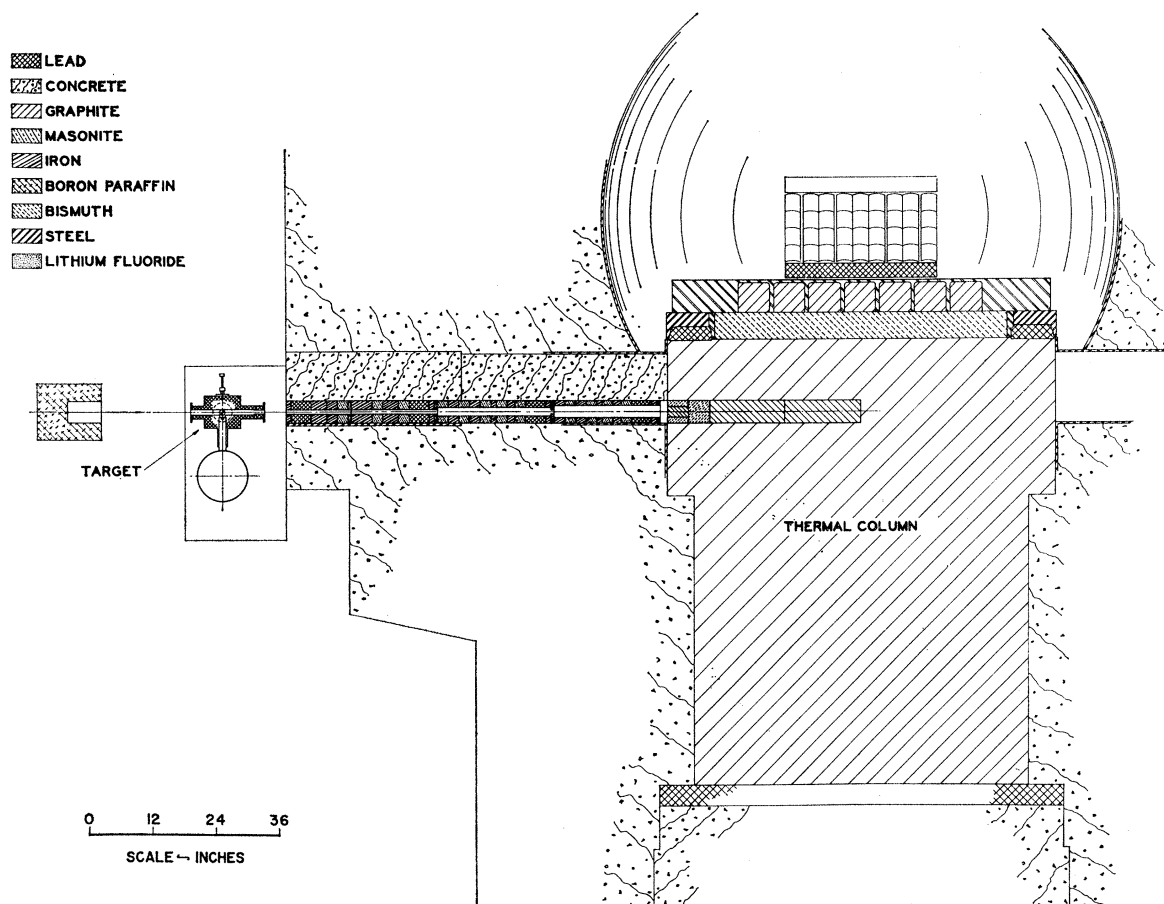


FIG. 1. Horizontal section of the reactor showing collimator for the external neutron beam and location of coincidence apparatus.

tive efficiency of the spectrometer at various low energies was determined by comparison with a NaI scintillator of known efficiency. With the energy dependence of the spectrometer efficiency thus known, the partial capture cross sections of the low-energy gamma-ray transitions in ^{60}Co were derived by extending the higher energy nitrogen calibration to low energies.

Data from these measurements were recorded by a 1600-channel pulse-height analyzer. The line areas and positions were determined by least-squares fitting of an appropriate Gaussian function to the data.

Capture Gamma-Ray Coincidence Measurements

The coincidence technique used for the study of the $^{59}\text{Co}(n,\gamma)$ reaction involves selection of a high-energy gamma-ray transition with a Ge(Li) detector and observation with a NaI detector of the low or moderate-energy radiation coincident with this transition. In effect, the high-energy transition from the capture state selects a definite low-energy level, the decay of which is then observed free from the background produced by the multitude of other radiations from the target.

For these measurements, a neutron beam, originating

in the reactor thermal column, was incident on a target placed outside the biological shield of the reactor (see Fig. 1). Such a neutron beam, originating in the graphite thermal column, is relatively free of gamma-ray contamination. To be present in the external neutron beam, gamma radiation originating in the reactor core must pass through a 7-in. lead and bismuth absorber located at the head of the thermal column and must then be scattered at an angle of about 90 deg. An additional 90-deg scattering is required to reach the detectors. The major background with this geometry is caused by neutrons which are scattered by the target itself.

The neutron beam, 3/8 in. in diameter, with an intensity of about 2×10^6 neutrons/sec, passes through an evacuated, shielded chamber (Fig. 2) containing the target and detectors. This Pb-filled chamber shields the detectors from room background and prevents inter-detector scattering events from contaminating the coincidence data. The shielding material in the neighborhood of the NaI detector is arranged to form a conical collimator so that only a central 1.5-in.-diam circle on the face of the 3-in. \times 3-in. NaI detector is illuminated by the target. Such collimation of the incident gamma rays significantly improves the spectral response of the

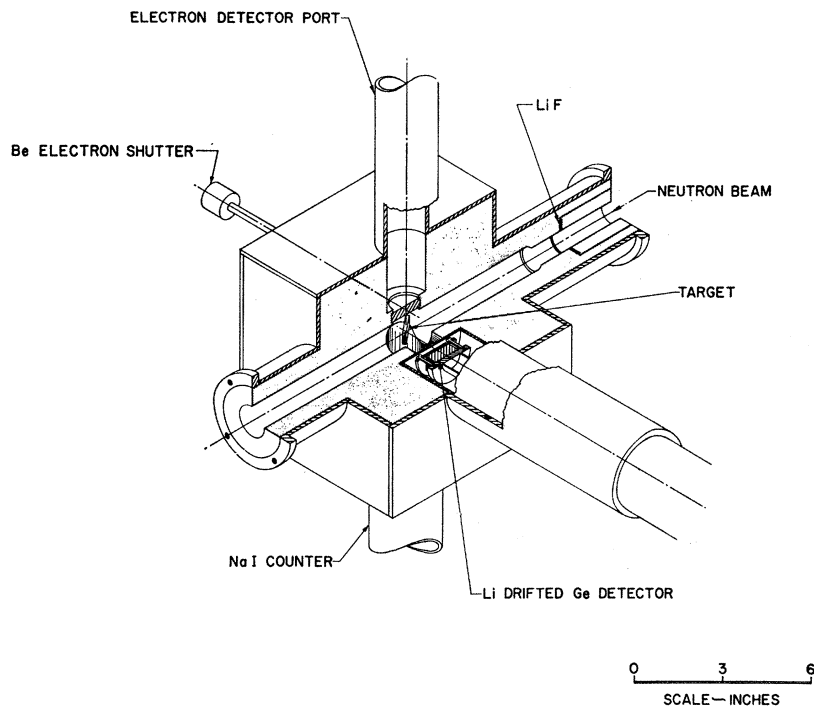


FIG. 2. Shielded chamber for coincidence measurements. The NaI scintillator views the target from below.

detector by reducing the probability that a Compton-scattered photon can escape from the crystal. The NaI detector and the 2.8-cm² by 4-mm Ge(Li) detector are shielded from the neutrons scattered by the target with thin Li⁶F-loaded ceramic absorbers. An additional port, illustrated in Fig. 2 but not used in this experiment, is provided for the study of neutron-capture internal-conversion spectra.

The coincidence data from the detectors are recorded event by event on magnetic tape by a two-parameter, 400×400-channel, multichannel analyzer. The tapes are read and the data are sorted and stored for further processing in the magnetic disk file of the Los Alamos MANIAC computer.

III. EXPERIMENTAL RESULTS

High-Energy Spectrum

The data shown in Fig. 3 are typical of several measurements of the high-energy capture gamma-ray spectrum from the ⁵⁹Co(*n*, γ)⁶⁰Co reaction. The highest energy line observed (No. 1) is at 7489.7±3.0 keV and corresponds to a transition directly to the ground state. This energy, which represents the neutron binding energy of ⁶⁰Co, is in good agreement with the value of 7486±11 keV derived from the ⁵⁹Co(*d*,*p*) studies.⁶ The excitation energies of the levels corresponding to the other high-energy gamma rays were derived by subtracting the observed transition energies from our quoted value of the binding energy. These are listed in Table I together with the primary gamma-ray energy

and the observed intensity. The excitation energies observed in the (*d*,*p*) studies are also indicated. An error of ±3 keV has been assigned to all of the primary gamma-ray energies since these values include any uncertainty in the ¹⁵N neutron binding energy upon which the energy calibration is based. All lines have been assigned the same error, since errors arising from uncertainty in the calibration are significantly larger than errors resulting from uncertainty in locating the line centroid, even for the weakest lines. The excitation energies, which involve only energy differences, are assigned a smaller error. If it is assumed that all the lines listed correspond to primary transitions, the sum of the intensities in Table I represent about 80% of the total (*n*, γ) cross-section.

Several of the observed lines corresponding to excitation energies greater than 1.2 MeV appear to consist of two or more unresolved components. These cases have been identified as "complex" in Table I, and the energy and intensity quoted are based on the line as a whole, without regard to the structure which may be present. The only complex peak present in the spectrum with an excitation energy less than 1200 keV is the one consisting of lines 3 and 4. The values pertaining to these two lines as listed in Table I are based on several runs which were made to clarify the structure of this doublet and to confirm the existence of line 2.

With the exception of the 738-keV level, all levels below 1.7 MeV identified in the (*d*,*p*) studies are also populated in the (*n*, γ) reaction by transitions leading directly from the capture state. For those levels which

TABLE I. High-energy capture gamma rays of ^{60}Co . The $^{60}\text{Co}(d, p)$ excitation energies are from Ref. 6.

Line number	Gamma-ray energy ^a (keV)	Intensity ($\gamma/1000 n$)	Excitation energy ^b (keV)	Excitation energy from $^{60}\text{Co}(d, p)$
1	7489.7	30.0± 5.0	0	0
2	7432.2	1.4± 0.5	57.5	58
3	7213.7	38.0± 6.4	276.0	282°
4	7201.6	11.0± 3.6	288.1	288.1
5	7055.4	16.0± 2.7	434.3	432°
6	6984.6	30.0± 5.1	505.1	501
7	6949.2	6.2± 1.8	540.5	541
8	6876.6	85.0± 14.0	613.1	612 738
9	6705.1	85.0± 14.0	784.6	783
10	6485.3	71.0± 11.6	1004.4	1006
11°	6278.2	12.7± 2.6	1211.5	1207
12	6148.9	3.7± 0.9	1340.8	1337
13	6111.0	5.0± 1.3	1378.7	1377
14	6040.9	5.9± 1.5	1448.8	1447
15	5976.0	73.0± 12.0	1513.7	1512
16	5925.8	17.0± 3.3	1563.9	...
17	5852.4	2.3± 0.68	1637.3	1638 1707
18	5743.3	23.0± 4.2	1746.4	1748
19	5705.1	3.6± 0.96	1784.6	...
20	5662.0	69.0± 11.0	1827.7	1799°
21	5640.1	14.1± 3.8	1849.6	1829
22	5617.1	11.7± 3.4	1872.6	1850
23	5604.6	15.0± 3.9	1885.1	...
24	5512.6	8.7± 2.2	1977.1	1887 1923
25°	5366.4	10.2± 2.4	2123.3	1979 2031
26	5272.1	11.5± 1.9	2217.6	2131
27	5213.7	5.2± 1.3	2276.0	2150
28	5182.7	36.0± 5.9	2307.0	2217
29	5151.2	3.3± 1.0	2338.5	2274
30	5129.3	6.6± 1.4	2360.4	2310
31	5069.1	5.0± 1.3	2420.6	...
32	5041.2	3.0± 0.88	2448.5	2348
33	5003.2	8.8± 1.6	2486.5	...
34	4963.7	2.6± 1.0	2526.0	...
35	4946.1	6.9± 2.0	2543.6	...
36	4922.2	9.7± 2.5	2567.5	...
37	4906.3	21.0± 3.9	2583.4	...
38	4885.7	17.0± 4.2	2604.0	2591
39	4724.6	4.4± 1.3	2765.1	...
40	4705.7	4.8± 1.2	2784.0	2734
41	4666.2	4.0± 1.0	2823.5	2762
42	4647.8	3.1± 0.85	2841.9	...
43	4607.1	8.8± 1.8	2882.6	...

^a $\Delta E = \pm 3$ keV.
^b $\Delta E = \pm 1.5$ keV.
^c Complex peak.

are populated by both reactions, a comparison of excitation energies shows excellent agreement. As already noted, the somewhat better resolution of the (n, γ) measurements permitted separate identification of lines 3 and 4. No evidence of complex structure was found for the level corresponding to line 5, which was identified as complex in the (d, p) studies.

Between 1.7 and 2.3 MeV, there are several states which are not populated by both reactions (see Fig. 9).

Above about 2.3-MeV excitation there is an almost complete breakdown in correspondence of the levels identified in the two studies.

There have been several previous studies of the high-energy capture gamma-ray spectrum of ^{60}Co . All have had inferior resolution compared to that presently available. The most recent of these earlier measurements was made by Wasson *et al.*,⁵ who used a Ge(Li) detector. For lack of independent high-energy calibra-

TABLE II. Low-energy capture gamma rays of ^{60}Co . The assignments shown the location in the level scheme of each transition. Confidence in the assignments is indicated by: (1) definite-coincidence evidence, (2) probable—not certain, (3) energetically possible.

Gamma-ray energy (keV) ($\Delta E = \pm 1.5$ keV)	Intensity ($\gamma/1000 n$)	Intensity error	Assignment ^a
58	> 17.0		58 → 0 (2)
159.0	61.0	11.0	434 → 276 (1)
195.8	6.2	1.3	738 → 540 (2)
218.8	2.0	0.8	276 → 58 (2)
229.6	210.0	35.0	288 → 58 (1)
254.1	23.0	3.9	540 → 288 (1)
276.9	120.0	20.0	276 → 0 (1)
336.8	2.7	0.6	613 → 276 (1)
349.5	1.7	0.5	785 → 434 (2)
390.9	81.0	13.0	1004 → 613 (1)
435.3	12.6	2.6	434 → 0 (1)
447.2	73.0	12.0	505 → 58 (1)
460.7	11.7	2.4	1004 → 540 (1)
483.7	16.6	3.4	540 → 58 (1)
496.7	50.0	8.0	785 → 288 (1)
511.0	22.0	4.6	anni. rad. (2)
555.7	98.0	16.0	613 → 58 (1)
600.9	1.3	0.4	1341 → 738 (3)
665.4	1.6	0.5	1449 → 785 (3)
680.0	5.3	1.3	738 → 58 (2)
710.4	15.6	3.3	1449 → 738 (3)
717.0	23.0	5.7	1004 → 288 (1)
726.9	18.0	3.0	1004 → 276 (1)
785.2	42.0	6.9	785 → 0 (1)
828.0 ^b	2.5	0.8	1563 → 738 (3)
854.0 ^b	2.4	0.8	1637 → 785 (3)
883.6	4.7	1.3	1885 → 1004 (3)
901.1	8.9	2.2	1514 → 613 (1)
929.8	13.3	2.8	2307 → 1379 (3)
944.9	21.0	4.5	1004 → 58 (1)
963.4	3.7	1.0	1746 → 785 (3)
1003.8	3.9	1.1	1004 → 0 (3)
1022.6	5.3	1.4	1564 → 540 (3)
1091.5	9.1	2.2	1379 → 288 (3)
1102.7	5.7	1.6	1378 → 276 (3)
1172.8	7.9	2.2	1449 → 276 (3)
1206.8	6.0	1.5	1746 → 540 (3)
1215.6	13.4	2.8	1828 → 613 (3)
1237.6	7.7	2.5	1514 → 276 (1)
1262.1 ^b	4.4	1.4	1873 → 613 (3)
1332.6	10.6	2.2	1873 → 540 (3)
1361.9	5.4	1.8	1637 → 276 (3)
1506.9	15.5	3.6	1564 → 58 (2)
1515.2	55.0	11.5	1514 → 0 (1)
1691.0	11.3	2.3	1746 → 58 (3)
1773.5 ^b	9.2	2.2	1828 → 58 (2)
1785.2	5.7	1.9	1785 → 0 (2)
1800.4	9.2	3.0	1779 → 0 (3)
1805.4	6.2	2.1	2544 → 738 (3)
1829.2	43.0	7.2	1828 → 0 (1)
1851.1	13.3	2.8	1850 → 0 (2)

^a Confidence.
^b Complex.

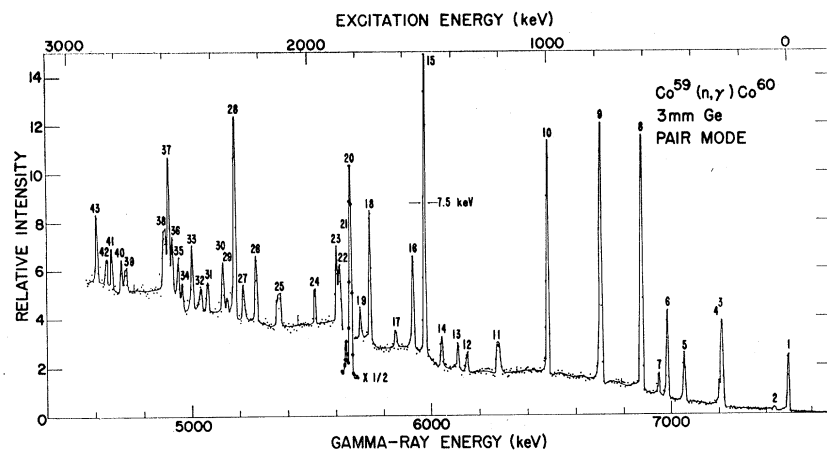


FIG. 3. High-energy portion of the gamma-ray spectrum from the $^{59}\text{Co}(n,\gamma)^{60}\text{Co}$ reaction, obtained with a 3-mm-deep Li-drifted germanium detector (see text).

tion standards, these authors used several of the excitation energies as determined from the (d,p) measurements as an energy calibration. The intensity calibration was based on the earlier work⁴ by Groshev and by Bartholomew. Because of their dependence on these earlier measurements, a precise comparison of our energy and intensity values with those of Wasson *et al.* is not presented here. Several of the lines identified by these authors have not been confirmed in our measurements. In particular, no evidence was found for states at 303, 1573, or 1798 keV.

Low-Energy Spectrum

The low-energy capture gamma-ray spectrum from the $^{59}\text{Co}(n,\gamma)$ reaction was measured over the energy range 50–1850 keV using the Ge(Li) detector surrounded by the anti-coincidence NaI annulus described earlier. The Co target and the geometrical arrangement were

identical to that employed in the high-energy spectral measurements.

A typical spectrum is illustrated in Fig. 4. In the energy range studied, 51 lines were observed. These are listed together with their intensities in Table II. Several of these lines have a complex structure which was not clearly resolved; such cases are noted in the table. In the region below 100 keV, the sensitivity of the spectrometer is strongly affected by absorption in the graphite target holder and the window of the Ge(Li) detector Dewar, through which the gamma-ray beam must pass before striking the detector. For this reason, only a lower limit is given for the intensity of the 58-keV transition.

The NaI anticoincidence annulus used in this measurement, while eliminating much of the Compton distribution associated with each of the lines, accentuates the sharpness of the high-energy edge of the Compton distribution. These edges arise from photons which are

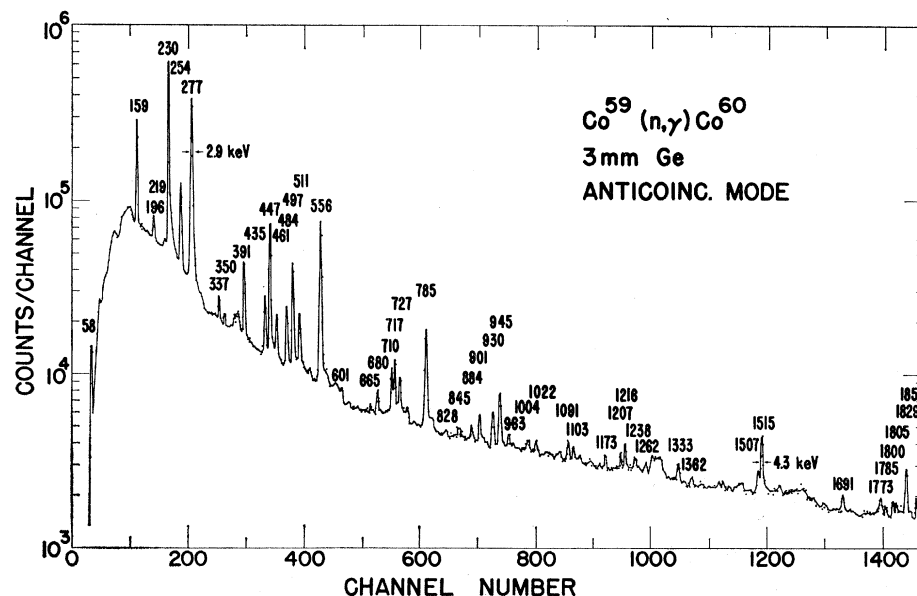


FIG. 4. Low-energy portion of the gamma-ray spectrum from the $^{59}\text{Co}(n,\gamma)^{60}\text{Co}$ reaction, obtained with a 3-mm deep Li-drifted germanium detector. The germanium detector was operated inside a large anti-coincidence NaI annulus (see text).

TABLE III. Relative intensities of transitions as observed in coincidence with the primary high-energy lines. Intensities are normalized to unity for the strongest line in coincidence with each primary transition. Blanks indicate that no coincidence was observed.

Line No.	3, 4	5	6	8	9	10	15	20, 21
Excitation energy (keV)	276	434	505	613	785	1004	1514	1828
	288							1850
Gamma-ray energy (keV)	→ 7213.7	7055.4	6984.6	6876.6	6705.1	6485.3	5976.0	5662.0
	7201.6							5640.1
↓								
159		0.8						
219	<0.08	<0.05						
230	0.4				0.8	0.9	0.4	0.4
254						0.2		
276	1.0	1.0		0.04		0.4	0.3	0.3
337				0.03		<0.2	<0.08	
391						0.8		
435		0.3						
447			1.0					
461						0.4		
484						0.2		
497					1.0			
505			<0.04					
556				1.0		1.0	0.2	
717						0.5		
727						0.5		
785					1.0			
901							0.2	
945						0.5		
1004						<0.1		
1238							0.2	
1515							1.0	
1773								<0.3
1829								1.0
1851								<0.6

backscattered from the detector and escape detection by the annulus as they travel back along the path of the incoming radiation. In the observed spectrum, these edges have the appearance of weak broad lines. Three such edges due to the strong 159-, 230-, and 277-keV lines are clearly visible in the region between the 159- and 58-keV peaks. Since the position of these edges is readily calculated, they do not present a serious problem in interpretation except to the extent that they obscure weak lines in their immediate vicinity.

Coincidence Measurements

The low-energy spectrum (energies < 2300 keV) was observed in coincidence with each of the reasonably strong high-energy lines. The Ge(Li) diode used as the high-energy detector in the coincidence measurements does not have the benefit of the surrounding NaI annulus and the background under the peaks is therefore considerably larger than that shown in Fig. 3. To reduce the contamination introduced into the coincidence data by this background, the following subtraction procedure was used. The low-energy spectrum in coincidence with a given high-energy line was formed by adding columnwise those rows of the coincidence matrix corresponding to the desired peak. Neighboring rows representing the spectral continuum were then subtracted. This procedure, which is possible when the entire two-dimensional coincidence matrix is recorded, is equivalent to the

“double-window” technique used when single-channel analyzers provide a coincidence gating signal from the selected transition. Typical coincidence spectra derived in this way are shown in Fig. 5. The bottom spectrum in Fig. 5 shows, for comparison, the complex singles spectrum obtained with the NaI detector. The simplification introduced by the coincidence requirement is readily apparent.

All spectra taken with the external target geometry show a peak at 511 keV caused by pair production in the shielding material which surrounds the target. These annihilation peaks also appear to some extent in the coincidence spectra, since two 511-keV quanta are produced each time a high-energy gamma ray is detected in the Ge(Li) counter. In spite of the shielding material between the detectors, some of these photons penetrate to the NaI detector and are recorded.

The results of the coincidence measurements are summarized in Table III, which lists the relative intensities of gamma rays seen in coincidence with each high-energy line. These intensities are normalized to unity for the most intense transition associated with a given high-energy line.

In many cases the relative transition intensities from the coincidence measurements as listed in Table III can be compared with relative-intensity information derived from the low-energy spectrum (Table II). Agreement between the two sets of values appears to be quite satisfactory. Once the level scheme is understood, the gamma-

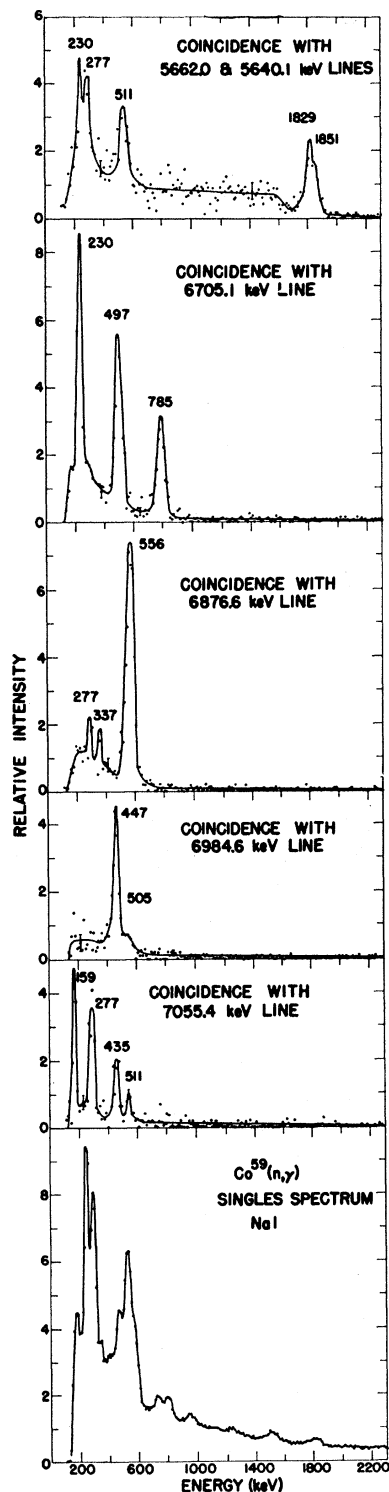


FIG. 5. Representative coincidence spectra obtained with a NaI scintillator. Coincidence gating signals were obtained from a Li-drifted germanium detector viewing the high-energy gamma-ray spectrum. The ungated spectrum obtained from the NaI detector is shown at the bottom for comparison. The simplification introduced by the coincidence requirement is readily apparent.

ray branching ratios derivable from the singles data are considered to be the more precise since these are based on superior counting statistics and do not involve effects arising from angular correlations of the gamma-ray cascades.

IV. INTERPRETATION OF EXPERIMENTAL RESULTS

Level Structure

The level scheme shown in Fig. 6 presents our interpretation of the coincidence data. The width of the arrows on the figure represents the intensity of the corresponding transition in the singles spectrum. Levels up to 1500 keV have been included in the figure. Although many levels have been identified above this energy, the coincidence data do not provide much additional information concerning the decay of these states due to the low intensity of the primary line and partition of this intensity into many decay branches.

For purposes of identification the levels have been assigned energy values based on the observed energy of the primary capture transition to that level. An independent set of level energies can be derived by appropriate combination of the observed secondary-transition energies. For the majority of levels, the two methods yield values which differ by less than 1 keV. We have not attempted to define a "best value" for each level energy by combination of the two sets of values.

Table II lists an assignment in the level scheme for each of the secondary transitions. Since there is considerable variation in our confidence in the different assignments, we have also included the estimated reliability of each assignment. The high-level density of the odd-odd ^{60}Co nucleus results in a very large number of secondary transitions. On the basis of the transition energy alone, there is usually more than one position in the level scheme to which a given transition might be assigned. However, the coincidence data uniquely define those which originate from the lower lying levels. In a few cases, insufficient counting statistics make the coincidence data somewhat ambiguous. For example, the weak 218.8-eV transition could arise between the 276- and 58-keV states, or perhaps between the 505- and 288-keV levels. Although the precise energy value somewhat favors the former, the available evidence does not permit a definite assignment. Similar considerations pertain to the 349.5- and the 460.7-keV transitions.

The levels at 738 and 540 keV are not populated directly from the capture state with sufficient intensity to obtain significant coincidence data concerning the decay of these states. The transitions shown as originating from these levels have been assigned solely on the basis of energy considerations.

Spin Assignments

Previous studies⁴ have shown that the spin and parity of the ground and first excited states of ^{60}Co are $5+$ and $2+$, respectively. Because of the large difference in spin between these two lowest states, it is possible to place limits on the spins of higher excited states by

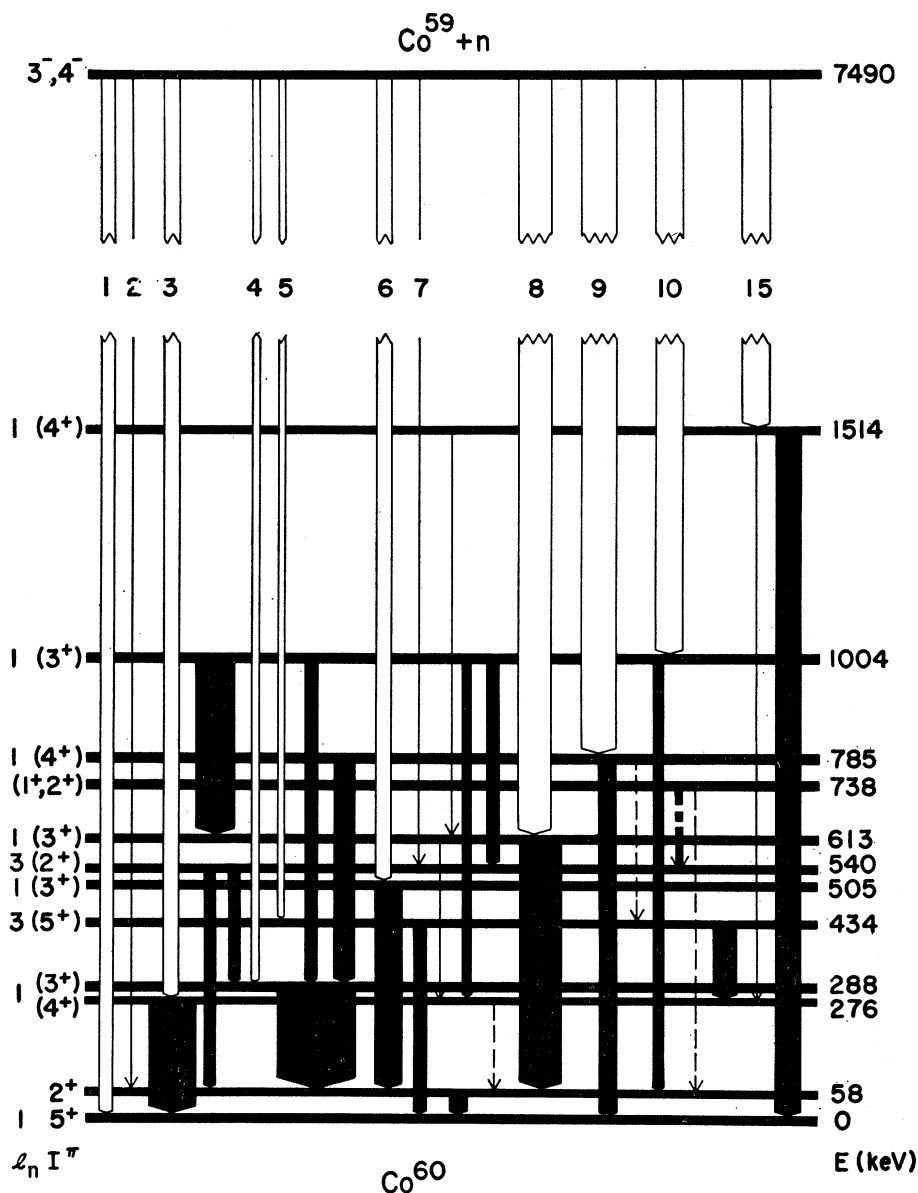


FIG. 6. Level structure of ^{60}Co . Gamma-ray intensities, represented here by the linewidth, were derived from the "singles" data. With the exception of some of the weak transitions (dashed lines), the location of all transitions in the scheme has been verified by the coincidence data.

observing to which of the two levels the higher states decay.

From the (d,p) -reaction angular-distribution measurements,⁶ the orbital angular momentum of the added neutron is known to be $l_n=1$ or 3 for the lower excited states. This leads to an assignment of positive parity for each of these levels. In this situation the strong low-energy transitions are expected to have $M1$ or mixed $M1$ - $E2$ character. Direct measurements⁴ indicate that the ground state of ^{59}Co has $I^\pi=7/2^-$. The compound state in ^{60}Co is therefore characterized by $I^\pi=3^-$ and 4^- . It is expected that the strong 132-eV, $J=4$ neutron-capture resonance will dominate thermal capture. In particular, the polarized-neutron measurements of Schermer⁹ have shown that about 78% of the thermal

capture is into the $I^\pi=4^-$ component. Therefore, from the capture state, primary $E1$ transitions are expected to proceed with greatest intensity to states of the latter three of the four possible spins, 2^+ , 3^+ , 4^+ , 5^+ . Direct population of a positive-parity state with spin outside this range would involve a transition of multipolarity $M2$ or higher, which would not compete with the faster $E1$ transitions.

The spins of the levels as shown in Fig. 6 were derived with the preceding considerations in mind. The principal guide in the assignment of spins has been to maximize the number of low-multipolarity ($M1$) transitions and to avoid the introduction of spin sequences which would imply obvious transitions that were not observed.

The more uncertain of the assignments are discussed individually below. Absence of a direct transition from

⁹ R. I. Schermer, Phys. Rev. 130, 1907 (1963).

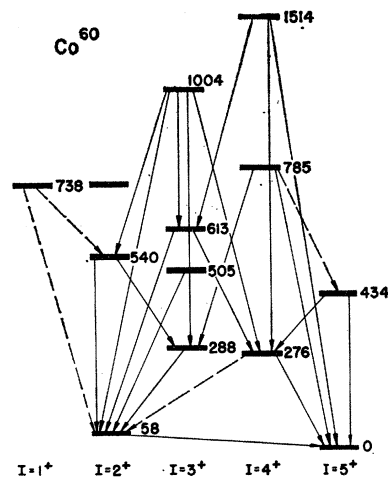


FIG. 7. ^{60}Co level schemes drawn with levels displaced horizontally according to proposed spins. Such a plot clearly shows that the observed gamma-ray transitions are consistent with the proposed spin assignments.

the capture state to the 738-keV level implies $I=0, 1,$ or 2 for the latter. Of these possibilities, the first is eliminated by the existence of the transition to the 540-keV level. We are left with the possibilities $I=1$ or 2 .

If the 738-keV state has $I=2$, the 540-keV level is permitted to have $I=2$ or 3 . The former possibility has been chosen since it is more consistent with the weak direct population of this state. A similar argument favors an $I=3$ assignment for the 505-keV level. The 434-keV state has been assigned $I=5$, rather than the possibility $I=4$, because of the absence of transitions connecting it with the 1004- and 288-keV levels.

The spin sequence derived above is self-consistent, and no $E2$ or higher multipolarity transitions are involved, with the possible exception of the weak and questionable 219-keV line connecting the 276- and 58-keV states. The consistency of the level structure is best illustrated by noting the observed transitions on a plot of level energy versus assigned spin as shown in Fig. 7.

V. DISCUSSION

The nucleus ^{60}Co has 27 protons and 33 neutrons. The shell model predicts that the proton configuration, consisting of one hole in the 28-particle closed shell, should be $\pi(1f_{7/2})^{-1}$. This configuration has been confirmed for ^{59}Co by the recent $^{58}\text{Fe}(^3\text{He},d)$ measurements of Blair and Armstrong.¹⁰ These authors have also shown that the first excited states of ^{59}Co at 1.10 MeV has $l=1$ and $I=3/2^-$, corresponding to the proton configuration $(2p_{3/2})^1$.

The single-particle neutron levels in the region $A=60$ have been discussed by Cohen *et al.*¹¹ From their study of deuteron stripping on the nickel isotopes, these authors conclude that the single-particle level ordering

in this region is $p_{3/2}, f_{5/2},$ and $p_{1/2}$ in order of increasing energy. The $p_{3/2}-f_{5/2}$ energy separation is about 400 keV in ^{61}Ni , while that of the $f_{5/2}-p_{1/2}$ orbitals is about 800 keV.

The ground-state spins of the odd- A , 33-neutron nuclei $^{59}\text{Fe}, ^{61}\text{Ni},$ and ^{63}Zn are all $3/2^-$, presumably resulting from the $\nu(f_{5/2})_0^2(p_{3/2})^{-1}$ configuration. Within the framework of the odd-group model we expect that the ground state and low-lying configurations of the odd-odd nucleus ^{60}Co can be described by the coupling of the $(f_{7/2})^{-1}$ proton hole and the $(p_{3/2})^{-1}$ neutron hole. Such a configuration will produce a set of levels with spins $2^+, 3^+, 4^+, 5^+$. The relative ordering of these states is sensitive to the nature of the residual proton-neutron interaction.

Historically, a variety of forms have been considered for the residual interaction. Theoretical understanding of odd-odd nuclei started with the empirical coupling rules which Nordheim¹² proposed to predict the ground-state spins of odd-odd nuclei. de-Shalit¹³ and Schwartz¹⁴ later showed that the success of the Nordheim rules could be understood by considering the interaction between the odd particle groups to be of the form

$$V_{pn} = -V_0[(1-\alpha) + \alpha(\boldsymbol{\sigma}_p \cdot \boldsymbol{\sigma}_n)]\delta(\mathbf{r}_p - \mathbf{r}_n), \quad (1)$$

where $\boldsymbol{\sigma}$ and \mathbf{r} are the nucleon spin and radial coordinates. The parameters V_0 and α specify the interaction strength and spin dependence. In the light of the $j-j$ coupling-model calculations of Schwartz,¹⁴ Brennan and Bernstein¹⁵ have reformulated the Nordheim rules to distinguish between particle-particle and particle-hole configurations. Using their revised coupling rules, Brennan and Bernstein successfully predict the spins of about 85% of the 76 low-lying levels considered. Exceptions are discussed by these authors in terms of configurations of higher seniority and configuration mixing. On the basis of their study, Brennan and Bernstein conclude that the spin-strength parameter α has a value of about 0.1. This value is consistent with that obtained for the free two-nucleon interaction. Vervier² has calculated energy spectra and binding energies of a number of nuclei in the range $50 \leq A \leq 58$ and finds good agreement with the experimental data using $\alpha=0.083$. The potential used in Vervier's work corresponds to $V_0 F_0 = 0.726$ MeV, where F_0 is a zero-order Slater integral.

To investigate a potential more physically realistic than the zero-range force of Eq. (1), calculations have been made using a finite range potential. Wells¹⁶ has calculated the energy spectrum of ^{60}Co using a potential which replaces the δ function of Eq. (1) with a radial

¹² L. W. Nordheim, Phys. Rev. **78**, 294 (1950).

¹³ A. de-Shalit, Phys. Rev. **91**, 1479 (1953).

¹⁴ C. Schwartz, Phys. Rev. **94**, 95 (1954).

¹⁵ M. H. Brennan and A. M. Bernstein, Phys. Rev. **120**, 927 (1960).

¹⁶ D. O. Wells, Nucl. Phys. **66**, 562 (1965).

¹⁰ A. G. Blair and D. D. Armstrong, Phys. Rev. **140**, B1567 (1965).

¹¹ B. L. Cohen, R. H. Fulmer, and A. L. McCarthy, Phys. Rev. **126**, 698 (1962); **133**, B955 (1964).

dependence of the form

$$f(r_{pn}) = (r_0/r)e^{-r/r_0}.$$

Despite the introduction of an additional parameter, use of this Yukawa-type interaction does not significantly improve the accuracy of the computed spectrum. A similar study by Ohnuma *et al.*¹⁷ has indicated that the residual interaction is very short range and is well approximated by the delta force.

Recently Rasmussen and Kim¹⁸ have investigated the effect of adding a tensor-force term to the residual interaction. Using parameters drawn from the free two-nucleon interaction for both central and tensor forces, these authors have calculated the level ordering for a number of odd-nucleon configurations. Although no major changes in level position are predicted in comparison with the purely central interaction, the relative ordering of neighboring levels is frequently changed. For example, the ground-state multiplet of ${}^{210}\text{Bi}$, which is incorrectly predicted by purely central forces, is satisfactorily explained by addition of a tensor interaction. We will refer to this work later in the discussion of the ${}^{60}\text{Co}$ level spectrum.

Most recently Kisslinger and Rote¹⁹ have investigated the constraints imposed on the form of a generalized residual interaction in order that it correctly predict the ground-state spins of a variety of spherical odd-odd nuclei. Using the quasiparticle representation and assuming only a single level for each odd nucleon, these calculations do not at present permit a detailed comparison with the ${}^{60}\text{Co}$ level structure.

For a preliminary analysis of the ${}^{60}\text{Co}$ level structure we used the zero-range interaction of Eq. (1) to calculate the states of lowest seniority, following the method of Schwartz.¹⁴ We wish to evaluate the matrix elements of the state with spin J , of the form

$$\langle j_1^{n_1} J_1, j_2^{n_2} J_2, J | V_{pn} | j_1^{n_1} J_1, j_2^{n_2} J_2, J \rangle, \quad (2)$$

where $j_i^{n_i} J_i$ represents n_i particles of spin j_i coupled to a resultant J_i . For the lowest seniority, $J_i = j_i$ and the energy of the coupled state J is

$$\begin{aligned} E((j_1)^{n_1} j_1 (j_2)^{n_2} j_2 J) \\ = V_0 \left\{ \left[\left(\frac{2j_1+1-2n_1}{2j_1-1} \right) \left(\frac{2j_2+1-2n_2}{2j_2-1} \right) E_w \right. \right. \\ \left. \left. - F_0 \left(n_1 n_2 - \left(\frac{2j_1+1-2n_1}{2j_1-1} \right) \left(\frac{2j_2+1-2n_2}{2j_2-1} \right) \right) \right] \right. \\ \left. \times (1-\alpha) + \alpha E_\sigma(j_1 j_2 J) \right\}, \quad (3) \end{aligned}$$

¹⁷ H. Ohnuma, Y. Hashimoto, and I. Tomita, Nucl. Phys. **66**, 337 (1965).

¹⁸ J. Rasmussen and Y. Kim, Akad. Nauk. SSSR **29**, No. 1 (1965); also Y. Kim, University of California Radiation Laboratory Report UCRL-10865 (unpublished).

¹⁹ L. S. Kisslinger and D. M. Rote, Phys. Rev. Letters **16**, 659 (1966).

where the energy is expressed in terms of the reduced energies $E_w(j_1 j_2 J)$ and $E_\sigma(j_1 j_2 J)$ for a pair of coupled particles. These quantities have been calculated by de-Shalit¹³ as

$$\begin{aligned} E_w(j_1 j_2) = -\frac{1}{2} F_0 (2j_1+1)(2j_2+1) (j_1 \frac{1}{2} j_2 - \frac{1}{2} | j_1 j_2 J 0)^2 \\ \times \frac{1}{2J+1} \left\{ 1 + \frac{[(2j_1+1) + (-1)^{j_1+j_2+J}(2j_2+1)]^2}{4J(J+1)} \right\} \quad (4) \end{aligned}$$

and

$$\begin{aligned} E_\sigma(j_1 j_2 J) = -\frac{1}{2} F_0 (2j_1+1)(2j_2+1) (j_1 \frac{1}{2} J_2 - \frac{1}{2} | j_1 j_2 J 0)^2 \\ \times \frac{1}{2J+1} \left[\frac{[(2j_1+1) + (-1)^{j_1+j_2+J}(2j_2+1)]^2}{4J(J+1)} \right. \\ \left. - [1 + 2(-1)^{j_1+j_2+J}] \right]. \quad (5) \end{aligned}$$

Ohnuma *et al.*¹⁷ have made a similar zero-range calculation for the $\pi(f_{7/2})^{-1} \nu(p_{3/2})^1$ configuration in ${}^{56}\text{Co}$. Fitting to the 4^+ , 3^+ , 5^+ and 2^+ levels of this nucleus at 0, 164, 501 and 984 keV, respectively, these authors find the best correspondence for strength and spin parameter values of $V_0 F_0 = 0.74$ MeV and $\alpha = 0.078$, respectively. Ohnuma has also calculated the ${}^{56}\text{Co}$ spectrum using a finite-range interaction. Such a calculation introduces an additional adjustable parameter $V_0 F_2$, where the F_2 radial integral reduces to $5F_0$ for the zero-range interaction. The best fit to the experimental spectrum occurs for $F_2 = 4.8F_0$, again indicating that the residual interaction is well approximated by the delta force.

Because of the good agreement obtained by Ohnuma for ${}^{56}\text{Co}$, we have used his parameter values in the present ${}^{60}\text{Co}$ calculation. Using Eqs. (3), (4), and (5) and normalizing to the ground-state energy we find the 2^+ , 5^+ , 3^+ , 4^+ levels of the $\pi(f_{7/2})^{-1} \nu(p_{3/2})^{-1}$ configuration of ${}^{60}\text{Co}$ lie at 0, 50, 470, and 830 keV, respectively. These levels are compared with the experimental spectrum in Fig. 8. The agreement is quite good except for inversion in the order of the closely spaced ground and first excited states. The presence of the configuration $\nu(f_{5/2})_0^2$ does not appear to perturb the normal $(p_{3/2})^{-1}$ structure appreciably. Vervier² has calculated the splitting of the $\pi(f_{7/2})^1 \nu(p_{3/2})^1$ configuration of ${}^{50}\text{Sc}$ using the zero-range force and slightly different parameter values. Since the calculation leads to the same result for either particle-particle or hole-hole configurations, his calculation is also appropriate to ${}^{60}\text{Co}$ and indeed agrees closely with our results.

The inversion of the 5^+ and 2^+ states in the calculated spectrum can perhaps be understood in terms of the recent tensor-force calculations of Rasmussen and Kim.¹⁸ In a general survey of odd-nucleon configurations, these authors have shown that for the $\pi(f_{7/2})^1 \nu(p_{3/2})^1$ configuration the effect of adding a tensor

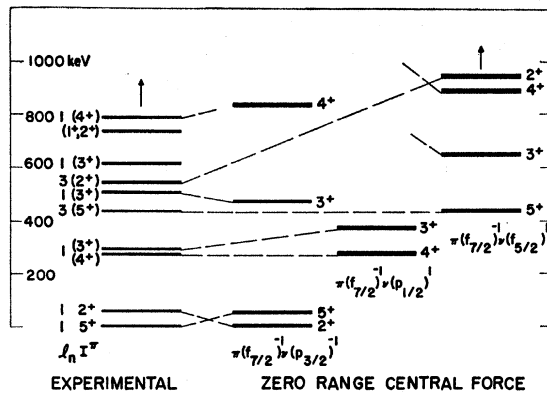


FIG. 8. Comparison of the experimental and theoretical energies of the low-lying states of ^{60}Co . A zero-range central force residual interaction with parameter values derived for ^{60}Co was used to calculate the level spacing for all three configurations. The inversion in the calculated order of two lowest states of the $\pi(f_{7/2})^{-1}\nu(p_{3/2})^{-1}$ configuration is discussed in the text. The levels at 276 and 288 keV, identified with the $\pi(f_{7/2})^{-1}\nu(p_{1/2})^{-1}$ configuration, are not believed to represent a major part of the $p_{1/2}$ neutron configuration in this nucleus.

component to a purely central interaction is to raise all the levels slightly (~ 50 keV), with the exception of the 5^+ state which is lowered in energy. These minor changes in level position are sufficient to make the 5^+ state become the ground state and the 2^+ level appear at approximately 50 keV. This is precisely the change required to bring our central-force calculation into agreement with the experimental ^{60}Co spectrum.

We note that the correct level ordering for the $\pi(f_{7/2})^{-1}\nu(p_{3/2})^{-1}$ configuration in ^{60}Co can be obtained without resorting to the tensor interaction. The calculated energies of the 5^+ and 2^+ states are degenerate for $\alpha \approx 0.1$, and for larger values of α the 5^+ state lies lowest, in agreement with the experimental observation. However, the calculated energy of the $I=4$ state is also increased by using a greater spin strength and the fit to the higher observed levels becomes somewhat worse. In the present analysis we have favored the tensor interaction interpretation since it retains the parameter values derived for ^{60}Co .

From the $p_{3/2}$ - $f_{5/2}$ single-particle neutron level spacing deduced by Cohen *et al.*,¹¹ we might expect states involving excitation of an $f_{5/2}$ neutron to occur above about 0.5 MeV in ^{60}Co . The lowest $l_n=3$ state, as identified by Enge,⁶ occurs at 434 keV and from our measurements appears to have $J=5^+$. We have calculated the level ordering of the $\pi(f_{7/2})^{-1}\nu(p_{3/2})^{-1}(f_{5/2})^1$ configuration using the zero-range interaction in the manner described previously, and find that indeed the $J=5^+$ level of this configuration should lie lowest. The calculated level ordering assuming $\alpha \leq 0.5$ is 5^+ , 3^+ , 4^+ , 2^+ , 6^+ , 1^+ . The 4^+ and 2^+ levels and the 6^+ and 1^+ levels are inverted at $\alpha \geq 0.16$ and $\alpha \geq 0.22$, respectively. Using the values of α and V_0F_0 employed in the $\pi(f_{7/2})^{-1}\nu(p_{3/2})^{-1}$ calculation and normalizing to the 434-keV, 5^+ state, we obtain the following energies for the $\pi(f_{7/2})^{-1}\nu(f_{5/2})^1$ configura-

tion: 434 keV (5^+), 649 keV (3^+), 885 keV (4^+), 945 keV (2^+), 1372 keV (6^+) and 2226 keV (1^+). There are a total of six levels which show strong $l_n=3$ stripping patterns [432, 541, 1799 (double), and 2348 keV], and presumably these states correspond to the six members arising from the $\nu(f_{5/2})^1$ configuration. The detailed energy agreement between these six levels and those calculated for the $\nu(f_{5/2})^1$ configuration is not particularly good. We do observe, however, that the total predicted splitting is approximately correct. Also the higher lying members are those which are not populated directly from the capture state as would be expected for levels with spins 1 and 6. Although the ^{60}Co parameters of Ohnuma have been used in this calculation, we note the proper level ordering for the $\pi(f_{7/2})^{-1}\nu(f_{5/2})^1$ configuration cannot be obtained with the interaction of Eq. (1) for any set of parameter values. The effect of the tensor interaction has not been explored for this configuration.

In addition to $p_{3/2}$ and $f_{7/2}$, the $p_{1/2}$ single-particle neutron level also occurs in the region of 33 neutrons. From the measurements of Cohen, this orbital appears about 1 MeV higher than the $p_{3/2}$ ground state. In the 33-neutron nucleus ^{61}Ni there is a spin- $\frac{1}{2}$ level at 284 keV, which presumably arises from the $p_{1/2}$ orbital. The pairing-model calculations of Kisslinger and Sorensen²⁰ in fact predict such a low-lying $I=\frac{1}{2}$ state arising from the $p_{1/2}$ configuration. We might expect to find such a level represented in ^{60}Co as a pair of states with spins $I=3^+$ and 4^+ . The residual interactions parameters appropriate for ^{60}Co predict that the $I=4$ level should occur about 80 keV lower than the level with $I=3$. A pair of states identified as $l_n=1$ and with the predicted spins are seen at 276 and 288 keV in ^{60}Co . Whether the above description is appropriate for these two states is not certain. For example, the spin- $\frac{1}{2}$ state in ^{61}Ni probably contains a large phonon component in order to appear at such a low excitation energy. It is probably that these two states, lying at such a low excitation energy, do not represent a major part of the total $p_{1/2}$ neutron amplitude in ^{60}Co . The preceding discussion does, however, provide a tentative interpretation of these two states.

Figure 9 shows a comparison of the levels populated by direct transitions from the capture state following the (n,γ) reaction with those excited by the (d,p) reaction. Wasson *et al.*⁵ have observed that there is no apparent correlation between the transition strengths for the two processes. The present measurements confirm this conclusion. Such correlations, sometimes found in other nuclei, have been interpreted as evidence of a basic similarity of the (n,γ) and (d,p) reaction mechanisms.

As we have noted, below 2.3 MeV there is almost a complete correspondence in levels excited by the two

²⁰ L. S. Kisslinger and R. A. Sorensen, *Rev. Mod. Phys.* **35**, 853 (1963).

reactions. Above 2.3 MeV there is almost no correspondence, with entirely different states being populated by the two reactions. Since the (d,p) reaction is expected to populate strongly only those levels which do not involve a change in the ^{59}Co ground-state proton configuration, while the (n,γ) reaction should show no such preference, we interpret this correspondence as possible evidence that the proton configuration is the same as that of the ground state for levels up to approximately 2 MeV. In the neighboring odd-proton nucleus ^{59}Co the excited proton configuration $p_{3/2}$ apparently occurs at about 1100 keV. We might therefore expect such states to appear in ^{60}Co at a similar excitation energy. We have no explanation for the implied "stability" of the ^{60}Co proton configuration.

An alternative hypothesis, which would explain the detailed correspondence of the (d,p) and (n,γ) excitations at low energies if not the breakdown at higher energies, is that the (n,γ) reaction populates only excited neutron configurations. Such a suggestion, which implies a direct-capture rather than a compound-nucleus capture state, has been proposed previously in studies²¹ of the deformed nuclei, ^{170}Tm and ^{166}Ho .

The apparent breakdown in correspondence between the two reactions above 2 MeV may suggest that the high energy (about 5.5 MeV) neutron-capture gamma rays assumed to be populating levels in this region directly from the capture state are, in fact, *not* primary. It is not unreasonable that some of the weaker of these transitions originate at levels in the neighborhood of 5 MeV.

VI. SUMMARY

Recent developments in the technology of Ge(Li) gamma-ray detectors have provided sufficiently good energy resolution (~ 7 keV) that the high-energy capture gamma-ray spectrum can be used to define the energies of a large number of the levels of the daughter nucleus.

Coincidence measurements using a Ge(Li) detector in combination with a NaI scintillator have been useful in specifying the de-excitation branches of the lower excited states and are a valuable adjunct to the spectral measurements. Knowledge of the mode of de-excitation of the lower excited states permits spin and parity assignments to be made for many of these levels. Probable spin values have been assigned to ten of the levels of ^{60}Co by this method.

²¹ R. K. Sheline, C. E. Watson, B. P. Maier, U. Gruber, R. H. Koch, O. W. B. Schult, H. T. Motz, E. T. Journey, G. L. Struble, T. V. Egidy, T. H. Elze, and E. Bieber, Phys. Rev. 143, 857 (1966); also H. T. Motz *et al.* (to be published).

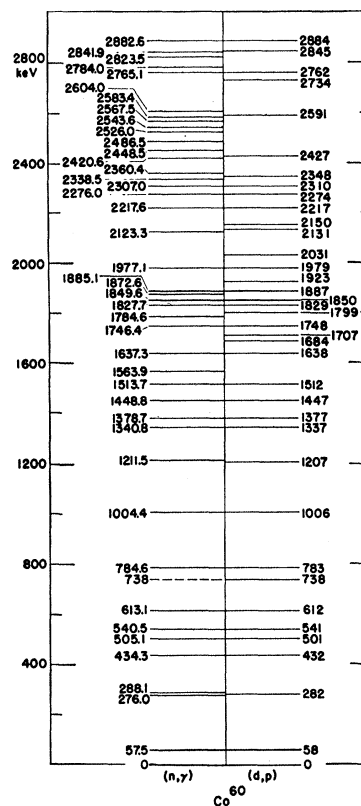


FIG. 9. Comparison of the states populated by direct transition from the capture state in the $^{59}\text{Co}(n,\gamma)$ reaction with those excited by the $^{59}\text{Co}(d,p)$ reaction.

The level energies and spin assignments of ^{60}Co have been compared with the predictions of the odd-group model using a zero-range central residual interaction. In spite of this somewhat superficial approach to the level structure of an odd-odd nucleus, reasonable agreement has been found, particularly for the lowest configuration, $\pi(f_{7/2})^{-1}\nu(p_{3/2})^{-1}$. The inversion of the two lowest states of this configuration, calculated with the central-force parameters derived for ^{56}Co , suggests the relevance of the recent tensor calculations of Rasmussen and Kim. A comparison of the levels populated by primary high-energy transitions from the capture state with those excited by the (d,p) reaction has provided information concerning the nature of these levels.

ACKNOWLEDGMENTS

The authors are grateful to E. T. Journey whose apparatus was used for the gamma-ray spectral measurements and to J. M. Palms who supplied the Ge(Li) detector used in the coincidence measurements. We are also grateful to M. E. Bunker, E. T. Journey, A. Kerman, H. T. Motz, and R. K. Sheline for helpful discussions.